Available online at www.sciencedirect.com
ScienceDirect
Journal of Electron Spectroscopy and Related Phenomena 156–158 (2007) 86–91
JOURNAL OF ELECTRON SPECTROSCOPY and Related Phenomena
www.elsevier.com/locate/elspec

Design and performance of an (e, e+ion) spectrometer for studies of fragmentation of dipole and non-dipole states of gaseous molecules

Glyn Cooper, Jacob Stewart-Ornstein, Adam P. Hitchcock *

Department of Chemistry, McMaster University, Hamilton, Ontario L8S 4M1, Canada

Available online 2 December 2006

Abstract

An (e, e+ion) spectrometer has been constructed that has the capability to measure time-of-flight (TOF) mass spectra of gases in coincidence with energy selected inelastically scattered electrons, as a function of impact energy, electron energy loss and electron scattering angle. Relative to earlier dipole-regime implementations of the (e, e+ion) technique, this spectrometer can be used to study molecular fragmentation under both dipole and non-dipole electronic excitation and ionization conditions. The spectrometer uses a position-sensitive electron detector and a TOF tube positioned at 90° with respect to the electron impact and scattering plane. The TOF design makes it possible either to extract all ions from the interaction region, or to discriminate preferentially for ions that have kinetic energy along the axis of the TOF tube, thus allowing one to collect spectra with maximum efficiency, or to study the dynamics of the production of the molecular and fragment ions. The design and construction of the spectrometer is described, along with preliminary results for ionization in the S 2p excitation and ionization region of SF_6.

Keywords: Time-of-flight mass spectrometer; Electron impact; Gas phase; SF_6; Electron-ion coincidence

1. Introduction

The electronic excitation of atoms and molecules above 6 eV [1] plays an essential role in many fundamental and technologically important processes, e.g. auroras and plasma-induced etching of materials. Ionic fragmentation of inner shell excited and ionized molecules is an expanding field of study [2] which yields information about ionization dynamics and possible selective X-ray photochemistry. Such data are of fundamental interest and help interpret photon stimulated ionic desorption from surfaces, which is critical to practical X-ray photochemistry and lithography. Lab based fragmentation studies are a time honoured component of this field. For example, Eland and co-workers have pioneered photoelectron-photoion (PEPICO), photoelectron-fluorescence (PEFCO), velocity imaging photoelectron (VIPCO), and electron time-of-flight (ETOF) spectroscopy using lab-based systems [3]. Bonham used non-coincidence electron impact mass spectrometry to study cross sections for dipole and non-dipole electron impact induced fragmentation of molecules [4–7], and ion–ion coincidence in the dissociative multiple ionization and fragmentation of molecules (without tagging the excitation electron) following pulsed electron ionization [8,9].

Electron energy loss spectroscopy, under varying experimental conditions of electron impact energy, energy loss and scattering angle, has the ability to excite not only the electric dipole-allowed transitions probed by light, but also electric quadrupole (and other higher-order electric multipole transitions) and spin-exchange excitations. For the past ∼12 years a program of variable angle (non-dipole) electron energy loss spectroscopy has been carried out at McMaster University [10–12] (in collaboration with researchers from Rio de Janeiro) using a unique, home-built spectrometer. Studies include high-resolution non-dipole inner shell spectroscopy (100 meV) [11] and variable impact energy, variable scattering angle studies of inner shell excitation intensities, resulting in quantitative generalized oscillator strengths [10,12]. In a parallel research program, a time-of-flight (TOF) mass spectrometer has been used, in conjunction with synchrotron radiation as the excitation source, to study core-excited molecules [2]. The energy dependence of photofragmentation processes of molecules provides detailed information on chemical bonding, photoioinzation dynamics and site and/or state selective fragmentation. State-selective photochemistry can be used to control chemical reactions and may be useful for making new materials or devices. For example, photofragmentation studies of SPF_3 [13] showed that loss of all

* Corresponding author. Tel.: +1 905 525 9104x24749; fax: +1 905 521 2773.
E-mail address: aph@mcmaster.ca (A.P. Hitchcock).

0368-2048/$ – see front matter © 2006 Elsevier B.V. All rights reserved.
doi:10.1016/j.elspec.2006.11.058

three fluorine atoms to produce SP^+ occurs predominantly with P 2p excitation, and not at all with S 2p excitation or ionization. In contrast, the S=P bond is much more readily broken with S 2p excitation, as evidenced by the production of PF_3^+, PF_3^{++} and the (S^+, PF_3^+) ion pair signals only following S 2p excitation. Studies of the polarization, angle, and kinetic energy aspects reveal details of the photo-fragmentation mechanism. If bond breaking in an energetic ionic fragmentation occurs before rotational randomization of molecular orientation, then the direction of preferential ion emission is determined by the transition symmetry. In SPF_3 [13], when the TOF detector is aligned perpendicular to the electric vector of the light the P 1s → e* transition dominates the S^+ partial ion yield spectrum, whereas when the TOF detector is rotated 90° to place it parallel to the electric vector, the P 1s → $14a_1$* transition becomes the strongest.

The construction of the (e, e+ion) equipment described in this work is intended to extend the previous synchrotron (which are intrinsically dipole experiments) and dipole (e, e+ion) measurements [14–16] into the non-dipole regime. This is the first (e, e+ion) coincidence spectrometer capable of detecting TOF coincidence mass spectra at specifically selected non-zero electron scattering angles. The present paper describes the construction of the TOF tube and the operation of the resultant (e, e+ion) coincidence spectrometer, followed by some early results on the dipole and non-dipole fragmentation of SF_6. The results presented here are preliminary, and are intended to illustrate the current performance of the instrument and discuss our current instrumental challenges, rather than to document the expected fully optimized performance.

2. Experimental

The electron spectrometer portion of the apparatus is the McMaster Variable Angle, High Resolution Electron Spectrometer (McVAHRES). This instrument has been described in detail in previous publications [17,18], including installation and performance of the position sensitive parallel electron detection system [19]. An ion TOF tube was added to this instrument in the vertical direction, orthogonal to the scattering plane of electron beam and the electron spectrometer. This necessitated construction of a new collision region and the TOF tube itself, along with implementation of the associated steady state voltages and detector and coincidence electronics for operation of the spectrometer in the (e, e+ion) coincidence mode. Schematic views of the resulting non-dipole (e, e+ion) spectrometer, both from the side and top, are shown in Fig. 1. The experimental geometry consisting of an electron scattering plane, detection of scattered electrons at varying angles, and the perpendicular TOF-tube and ion detector, can be seen clearly. The spectrometer incorporates both a direct and a monochromated electron beam source, but for the present experiments, only the direct electron gun was used. Energy resolution for the electron spectrometer is typically ∼0.7 eV using electron beam from the direct (unmonochromated) electron gun, while ∼50 meV resolution has been achieved using the monochromated electron source. The effective acceptance angle of the electron analyzer varies with scattering angle from ∼1° at scattering angles ≤4° to ∼0.2° for scattering angles ≥80°, as documented in Ref. [19]. This very small angular acceptance limits the overall efficiency of the (e, e+ion) system. Changes to the electron optics to increase the acceptance angle are planned.

In basic form, the coincidence detection is started by detection of an energy loss electron at the position-sensitive electron detector, followed (usually some microseconds later) by detection of one or more positive ions by the ion detector. The detector is a Burle Instruments model APTOF40 with "fast" channel plates. Coincidence detection is provided by a multi-stop time-to-digital-converter (TDC) (Ortec model 9308), the signals for which are fast pulses taken from the back of the rear channel plate of the electron detector, and from the solid anode of the ion detector. These fast pulses are amplified (Ortec VT120A) and conditioned by constant fraction discriminator units (Ortec model 473A) before being fed to the TDC. The originating position of the detected electron (and hence its energy loss) can be obtained from a position sensitive detector (PSD, Quantar model

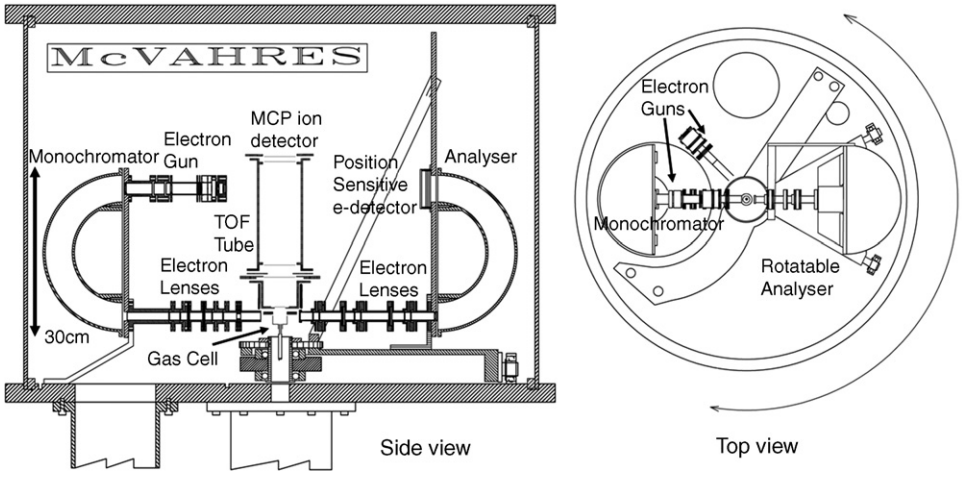

Fig. 1. Overview diagram of the McVahres spectrometer, showing side view (left hand side) and top view (right hand side). The experimental geometry can be clearly seen. For the present experiments, the non-monochromated electron gun source was used.

2502A) which is incorporated into the overall data-acquisition scheme. The position sensitive nature of the electron detector should give a significant performance boost to the data collection compared with single channel electron detection. However, the PSD does not store time-of-detection information, so in order to obtain coincidence data in an electron energy loss sensitive manner, it is necessary to read out the whole memory contents of the PSD for each coincidence detected. This operation takes ∼0.05 s, so the maximum coincidence count rate possible under electron energy sensitive conditions is ∼10 Hz or so. The other mode of operation is to treat the whole position sensitive detector as a single channel detector, in which case the energy loss sampled in the (e, e+ion) coincidence spectra corresponds to the energy width across the whole detector. This is ∼5 eV under typical electron analyzer pass energies, and in some cases such a large energy sampling is desirable, e.g. when collecting data for an electron energy loss band that has large natural width. Also, the electron count rate is often less than 10 Hz at inner shell energy losses, so that this is not such a serious limitation in practice. We are presently implementing an event-by-event position sensitive computing system (effectively by-passing the Quantar electronics) which will enable higher (e, e+ion) event rates with full use of the parallel energy loss system.

The design of the TOF tube and ion draw-out region was based on existing TOF instrumentation used for synchrotron dipole photoionization studies [20]. However, the dimensions of the tube and details of the ion draw-out functioning were modified in order to provide an optimal match with the variable angle electron energy loss spectrometer and the coincidence operation. Fig. 2 shows the collision region and TOF tube in cross section. Also shown are ion trajectories through the tube calculated using the SIMION [21] simulation program using the voltages shown. In practice all the voltages can be independently adjusted to optimize for different types of experiment. The ion paths shown are generated from three sets of positive ions, each set originating 3 mm apart along the electron beam direction, with five ions generated within each set, each of these having 20 eV kinetic energy over a range of ejection angles (0°, 72°, 144°, 216°, 288°). This diagram shows that under the voltage conditions shown, there should be complete collection of the positive ions produced with up to at least 20 eV kinetic energy of fragmentation along a 6 mm ionization "line" (which corresponds to the ionizing electron beam path in front of the TOF tube entrance). Variation of the draw-out voltage, the lens voltage and the TOF tube voltage leads to rather different ejected ion trajectories, such that experiments can be optimized to preferentially detect thermal ions, for example. A detailed description of the different kinds of experiments that are possible with the design of TOF tube employed in the presently described spectrometer can be found in Ref. [20].

Initially, we intended to use pulsed ion draw-out [23,24], which would have allowed a straight incident electron beam path through the collision region. However, it was found that this experimental mode was not practical, since the electron-ion coincident nature of the experiment was lost due to the high voltage draw-out pulse, and hence the positive ions detected were time-correlated with all the electron energy loss events, due to the pulsed draw-out field. Therefore, we used a static ion draw-out field, which provided good ion collection but deflected the incident electron beam path through the collision chamber. In order to compensate for the latter, additional electron deflectors were added before and after the collision region. In addition, extra shielding was needed around the collision chamber/drawout field region to avoid any influence of the drawout field on the electron beam except in a controlled manner inside the gas cell. This approach is similar to that used in the earlier (e, e+ion) coincidence apparatus [14–16,22].

Fig. 3 shows the arrangement used in the present work and the resultant electron beam path. The construction can be described as an electron double deflection arrangement, since the electrons are deflected in the same direction, by approximately the same amount, both before and after the collision chamber. The deflection is usually almost the same before and after the gas cell since the energy loss being studied is usually a small fraction (<10%) of the total incident beam energy, E_0 (e.g. for the SF_6 S 2p studies reported below, $E_0 \approx 2.0$ keV, energy loss ≈ 180 eV), therefore the electron beam energy is almost the same before and after the collision region. This double deflection scheme has proved to be a critical component of the operation of the spectrometer in the (e, e+ion) coincidence mode. Indeed, the coincidence signal rate is vanishingly small unless this system is tuned optimally. This is in addition to the rather stringent conditions of electron beam tuning in the McVahres spectrometer [17,18].

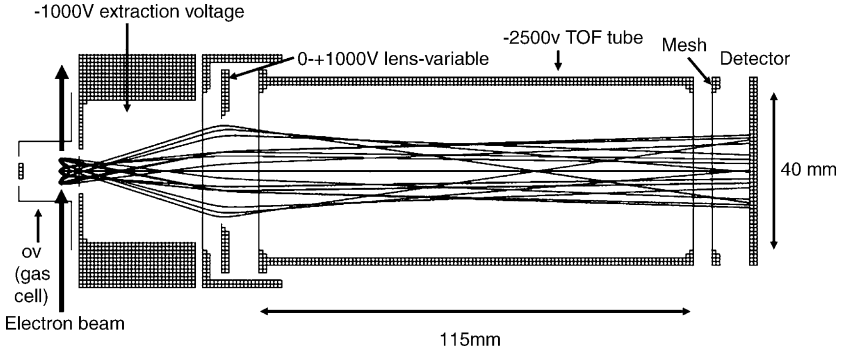

Fig. 2. Time-of-flight tube design and typical operational voltages. Simulated [20] ion trajectories through the tube, from collision region to detector, are also shown by the solid lines (see text for details).

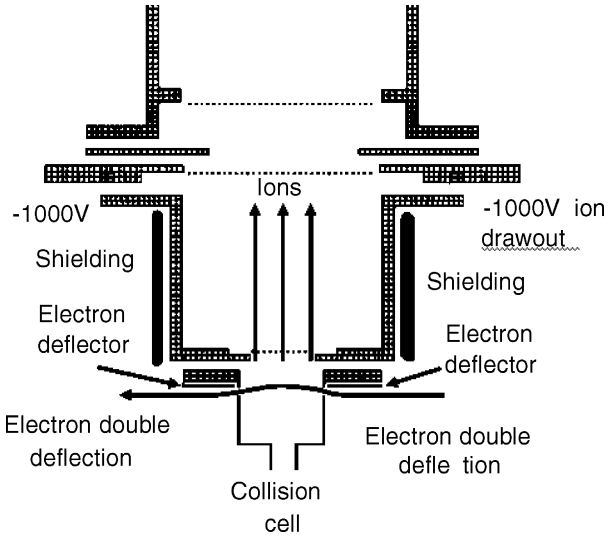

Fig. 3. Detail of the collision region and ion draw-out design. Also shown are the electron double deflection plates and the resultant electron trajectory through the collision region.

The gaseous sample of SF_6, of stated purity 99.8%, was obtained commercially from Liquid Carbonic Ltd. and was used directly.

3. Results and discussion

Fig. 4 shows two (e, e+ion) time-of-flight mass spectra of SF_6 (first stops only) collected at 40 and 100 eV electron energy loss and 2° electron scattering angle. The spectra took 10 min (40 eV) and 1 h (100 eV) to collect. One can see that for data of reasonable quality, for the valence shell and even up to ~100 eV in favorable cases (such as SF_6 which has a large scattering cross section at high energies) the collection of a set (or subset) of TOF data close to the dipole limit (close to 0° scattering angle) will take of the order of a few days using the instrumentation in its present form and condition. This time frame is similar to the

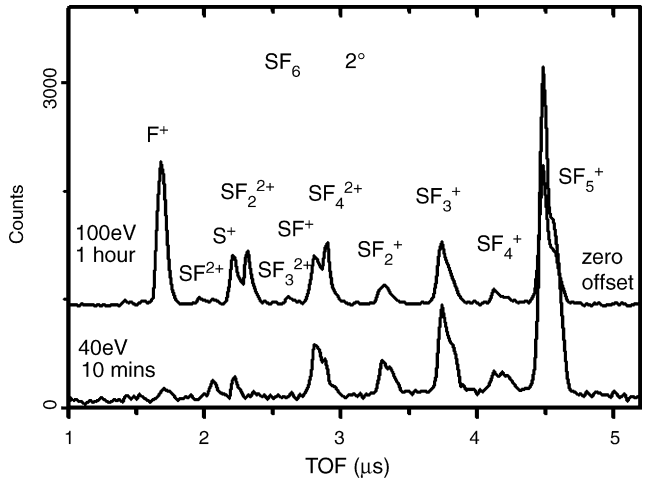

Fig. 4. Time-of-flight (e, e+ion) coincidence spectra of SF_6 recorded in the present work at 2° scattering angle and 100 eV (top plot) and 40 eV (bottom plot) electron energy loss.

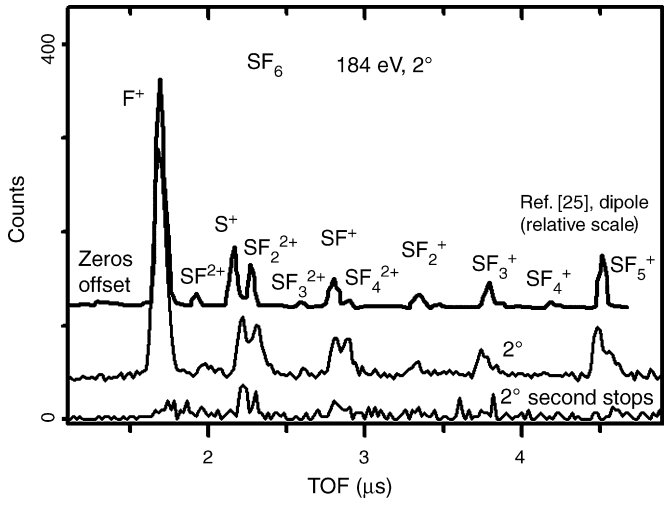

Fig. 5. Time-of-flight (e, e+ion) coincidence spectra of SF_6 at 184 eV electron energy loss. The dipole data are taken from Ref. [25], the 2° data are the present work.

time taken for data collection using the previous dipole (e, e+ion) spectrometer [25]. However, we should expect a faster data rate in the present experiment due to parallel electron detection. This is discussed in more detail below.

Fig. 5 presents an (e, e+ion) time-of-flight mass spectrum of SF_6 (first and second stops) collected at 184 eV electron energy loss and 2° electron scattering angle, in comparison with the previous (e, e+ion) mass spectrum [25] collected under dipole-dominated kinematic conditions (0°). The data are of comparable quality, but the present data took ~70 h to record, versus ~10–20 h for the earlier dipole data [25]. Since the new apparatus incorporates a position sensitive electron detector, one would expect the data accumulation to be more efficient since coincidence events over a range of energy losses are being simultaneously detected; however, this is obviously not the case. Based on the total electron count rate over the position sensitive detector and the electron-ion coincidence rate for the whole energy width sampled, we estimate ~30% for the detection efficiency of the TOF tube/detector. To explain the sensitivity reduction between the earlier dipole (e, e+ion) apparatus [25] and the present instrument, there must be a serious loss of detection efficiency in the electron channel and/or in the overlap of the electron and ion channel sampling volume. This is possibly due to non-optimal mechanical or electrical (beam deflection) alignment between the electron and ion channels, and if so this is something that can be addressed in the future. Another possibility is that the electron transport and focusing lenses between the collision region and the electron analyzer (see Fig. 1) are of low efficiency and/or are being operated in a low efficiency mode (despite being set in a focused condition). Recent changes to the analyzer entrance lens and larger apertures have resulted in a ~10-fold increase in efficiency in the electron detection efficiency with negligible adverse effects on energy resolution.

Fig. 5 shows that there is good qualitative agreement between the earlier dipole data [25] and the present first stop data taken at 2° scattering angle (close to dipole conditions), except for a few of the fine spectral details. In addition almost all of the

quantitative aspects of the spectra are very similar, i.e. the relative intensities of the various ion peaks observed are almost the same in the two data sets. The spectra do seem to differ somewhat in that the present data contain much more SF_4^{2+} intensity, and the SF_3^+ and SF_5^+ peaks are significantly more asymmetric in the present data (they have secondary peaks or "tails" towards higher time-of-flight (*m/e*)). The latter features may indicate something about the kinematics of the dissociation processes occurring after S 2p excitation in SF_6 at 184 eV, but further experiments utilizing different ion flight conditions (e.g. a different extraction and/or TOF tube voltage) are needed to verify this speculation. This comparison indicates that our experimental apparatus and conditions are capable of producing quantitative fragmentation (branching ratio) measurements. Corroboration of this is one of the goals for near future work with the spectrometer.

Information additional to that which could be obtained from the dipole (e, e+ion) TOF spectrometer [14–16,22] is provided in the present experiments by the second stop spectrum that is detected simultaneously with the main first stop spectrum. The true second stop signal arises from dissociative double ionization events which have produced a pair of ions from one ionization event. Careful analysis of the (e; e, ion–ion) signals, which are analogous to PEPIPICO in a synchrotron photoionization study, can reveal exquisite details of the photofragmentation process [2]. For SF_6, the multiple ionization events, as represented by the second stops data, constitute ∼11% of the overall ionization processes at 184 eV energy loss at 2° scattering angle. It is possible to identify S^+, SF_2^{2+}, SF^+, and possibly SF_4^{2+}, SF_3^+ and SF_5^+ peaks in the spectrum (Fig. 5). The S^+ and SF_2^{2+} species are the largest peaks and are the dominant ions produced along with F^+ in ion pair formation under these experimental conditions. Data with improved signal-to-noise ratio and a better trues-to-accidentals ratio are needed before we can begin to analyze in detail (e; e, ion–ion) triple coincidence signals. We note that the previous (e, e+ion) apparatus was not capable of multi-stop coincidence detection and thus this is a unique feature of the present instrument.

As shown in Fig. 6 a, there are dramatic changes in the SF_6 electron energy loss spectrum around 184 eV energy loss as the scattering angle is increased away from the dipole limit [17,26]. In particular, the transitions that compose the band centered around this energy, which are from the S 2p orbitals to the $B(t_{1u})$ and the T_{1u} (t_{2g}) states, change their relative intensities many-fold (see in particular Fig. 1 of Ref. [26]). At low momentum transfer, which corresponds to the 2° TOF spectrum recorded in the present work, the lower energy (∼181 eV) $B(t_{1u})$ state peak is of very low relative intensity, <5% of the intensity of the higher energy (∼184.5 eV) T_{1u} (t_{2g}) state peak, whereas at higher momentum transfers, the $B(t_{1u})$ state peak dramatically increases in relative intensity (Fig. 6a). At very high momentum transfer [26] (∼110 a.u., ∼60° scattering angle), the $B(t_{1u})$ state peak becomes more than twice as intense as the T_{1u} (t_{2g}) state peak. At the 11° scattering angle employed in the present work, the intensity of the $B(t_{1u})$ state peak is ∼20% of the intensity of the $T_{1u}(t_{2g})$ state peak [17]. Note that the energy resolution of the (e, e+ion) TOF spectra reported in this work is such that coincidences should appear in the 184 eV electron energy loss TOF spectra from production of both the $B(t_{1u})$ and $T_{1u}(t_{2g})$ states. Fig. 6b shows (e, e+ion) time-of-flight mass spectra of SF_6 (first and second stops) collected at 184 eV electron energy loss at both 2° and 11° electron scattering angle. The data taken at 11° is of lower signal-to-noise ratio despite the fact it was acquired over a much longer time (∼300 h versus 70 h). This is due to the great fall-off in electron energy loss intensity at higher scattering angles (due to the shape of the Bethe surface for this process [27–29]) and the fact that the TOF detects ions produced from all possible electron energy loss events that can take place from the incident beam, all of the time. Our coincidence experiment therefore becomes more and more reminiscent of the "needle in a haystack" problem as the scattering angle is increased. Singles count rates cannot be increased too high otherwise accidental coincidences overwhelm the real coincidences that we are attempting to detect. Nevertheless, if we have stable spectrometer conditions we can average signal over long time periods. Within experimental uncertainty, there are not any dif-

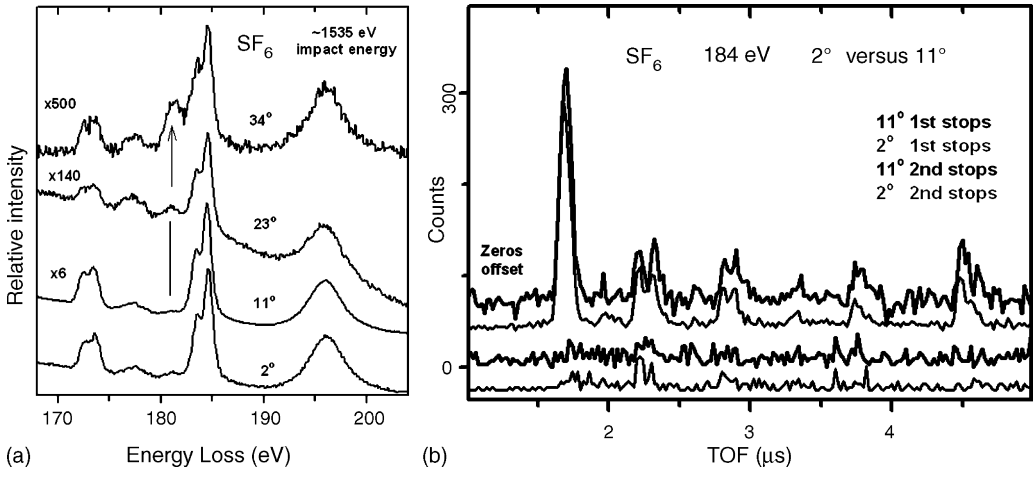

Fig. 6. (a) Electron energy loss spectra in the S 2p region of SF_6 at scattering angles of 2°, 11°, 23° and 34°, recorded with McVAHRES. (b). Time-of-flight (e, e+ion) coincidence spectra of SF_6 collected in the present work at 184 eV energy loss and 2° and 11° electron scattering angle. From top to bottom the spectra are: 1st stop spectrum at 11°, 1st stop spectrum at 2°, 2nd stop spectrum at 11°, 2nd stop spectrum at 2°.

ferences between the TOF data collected at 2° and 11° (Fig. 6). It appears that electron energy loss scattering angles higher than 11°, where the $B(t_{1u})$ state peak is more dominant in the electron energy loss spectrum, will be required to observe changes in the fragmentation pattern of S 2p core excited SF_6 with change in scattering angle, if indeed such differences exist. Future work will attempt to collect (e, e+ion) TOF spectra at these higher angles.

4. Summary

We have reported the construction of and preliminary results from an (e, e+ion) spectrometer which is designed for studies of fragmentation of non-dipole valence and inner-shell excited and ionized states of gaseous molecules. The TOF design is versatile and capable of both quantitative and ion dynamics studies. At present the instrument uses a static ion draw-out field and double deflection of the electron beam in the collision chamber. Comparison of preliminary results for SF_6 at 2° electron scattering angle with previous dipole (e, e+ion) data [25] shows that the quantitative design goal has been approached. Future work will focus on improving the efficiency of the electron channel, quantitatively characterizing the TOF system, and possibly optimizing a pulsed field ion extraction approach triggered by individual energy loss events. With such improvements we expect to be able to measure inner shell fragmentation at much higher electron scattering angles.

Acknowledgements

This work was supported financially by NSERC (Canada) and the Canada Research Chair program.

References

[1] R.L. Platzman, Rad. Res. 17 (1962) 419.
[2] A.P. Hitchcock, J.J. Neville, in: T.K. Sham (Ed.), Chemical Applications of Synchrotron Radiation, World Scientific, 2002, p. 154.
[3] D. Aitchison, J.H.D. Eland, Chem. Phys. 263 (2001) 449.
[4] C. Ma, C.R. Sporleder, R.A. Bonham, Rev. Sci. Instrum. 62 (1991) 909.
[5] C. Ma, M.R. Bruce, R.A. Bonham, Phys. Rev. A 44 (1991) 2921.
[6] C. Ma, M.R. Bruce, R.A. Bonham, Phys. Rev. A 45 (1992) 6932.
[7] M.R. Bruce, R.A. Bonham, Z. Phys. D 24 (1992) 149.
[8] L. Mi, R.A. Bonham, J. Chem. Phys. 108 (1998) 1904.
[9] L. Mi, R.A. Bonham, J. Chem. Phys. 108 (1998) 1910.
[10] A.P. Hitchcock, J. Electron Spectrosc. Relat. Phenom. 112 (2000) 9.
[11] J.T. Francis, N. Kosugi, A.P. Hitchcock, J. Chem. Phys. 101 (1994) 10429.
[12] A.P. Hitchcock, S. Johnston, T. Tyliszczak, C.C. Turci, M. Barbatti, A.B. Rocha, C.E. Bielschowsky, J. Electron Spectrosc. Relat. Phenom. 123 (2002) 303.
[13] J.J. Neville, T. Tyliszczak, A.P. Hitchcock, A. Jürgensen, R.G. Cavell, Chem. Phys. Lett. 300 (1999) 451.
[14] R.B. Kay, Ph.E. van der Leeuw, M.J. Van der Wiel, J. Phys. B 10 (1977) 2513.
[15] R.B. Kay, Ph.E. van der Leeuw, M.J. Van der Wiel, J. Phys. B 10 (1977) 2521.
[16] C.E. Brion, Comm. At. Mol. Phys. 16 (1985) 249.
[17] I.G. Eustatiu, J.T. Francis, T. Tyliszczak, C.C. Turci, A.L.D. Kilcoyne, A.P. Hitchcock, Chem. Phys. 257 (2000) 235.
[18] I.G. Eustatiu, T. Tyliszczak, A.P. Hitchcock, C.C. Turci, A.B. Rocha, C.E. Bielschowsky, Phys. Rev. A 61 (2000) 042505.
[19] A.P. Hitchcock, S. Johnston, T. Tyliszczak, C.C. Turci, M. Barbatti, A.B. Rocha, C.E. Bielschowsky, J. Electron Spectrosc. Relat. Phenom. 123 (2002) 303.
[20] A.C.O. Guerra, J.B. Maciel, C.C. Turci, R.C. Bilodeau, A.P. Hitchcock, Can. J. Chem. 82 (2004) 1052.
[21] D.A. Dahl, SIMION 3D. Version 6.0 [computer program]. Ion Source Software, PO Box 2726. Idaho Falls, ID 83403.
[22] X. Guo, G. Cooper, W.F. Chan, G.R. Burton, C.E. Brion, Chem. Phys. 161 (1992) 453 (and refs. therein).
[23] T.A. Field, J.H.D. Eland, Meas. Sci. Technol. 9 (1998) 922.
[24] E. Kukk, R. Sankari, M. Huttul, A. Sankari, H. Aksela, S. Aksela, J. Electron Spectrosc. Relat. Phenom., SCASM special issue (2007), in press.
[25] A.P. Hitchcock, C.E. Brion, M.J. Van der Wiel, J. Phys. B 11 (1978) 3245.
[26] I.G. Eustatiu, T. Tyliszczak, A.P. Hitchcock, Chem. Phys. Lett. 300 (1999) 676.
[27] H. Bethe, Ann. Phys. (Leipzig) 5 (1930) 325.
[28] H. Bethe, Z. Phys. 76 (1932) 293.
[29] H.F. Wellenstein, H. Schmoranzer, R.A. Bonham, T.C. Wong, J.S. Lee, Rev. Sci. Instrum. 46 (1975) 92.